

List of Figures:

Fig. 1:

Oxygen and Carbon concentrations in substrates investigated by the RD48/ROSE Collaboration.

Fig. 2:

Oxygen-concentration profiles for standard and oxygen enriched FZ silicon wafers as measured by SIMS.

Fig 3a:

Fluence dependence of leakage current for detectors produced by various process technologies from different silicon materials. The current was measured after a heat treatment for 80 min at 60°C [9]

Fig 3b:

Current related damage rate α as function of cumulated annealing time at 60°C. Comparison between data obtained for oxygen diffused silicon and parameterisation given in Ref. [9].

Fig 4a:

Dependence of N_{eff} on the accumulated 1 MeV neutron equivalent fluence for standard and oxygen enriched FZ silicon irradiated with reactor neutrons (Ljubljana), 23 GeV protons (CERN PS) and 192 MeV pions (PSI).

Fig 4b:

Effective space charge density and full depletion voltage versus proton fluence for standard, carbon-enriched and three types of oxygen diffused samples: 24, 48 and 72 hour diffusion at 1150°C.

Fig 5a:

24 GeV/c proton irradiation of O-rich diodes with different resistivity.

Fig 5b:

Reactor neutron irradiation of O-rich diodes with different resistivity.

Fig 6

Annealing behaviour of the radiation induced change in the effective doping concentration ΔN_{eff} at 60°C [9].

Fig 7:

Systematic analysis of annealing data. Change of effective doping concentration ΔN_{eff} during isothermal annealing at 60°C of oxygen enriched silicon detectors irradiated with different neutron fluences.

Fig 8a:

Stable Damage component N_C for neutron irradiated oxygen enriched silicon

Fig 8b:

Reverse Annealing N_Y for neutron irradiated oxygen enriched silicon

Fig 9a:

Damage parameters N_C for oxygenated and standard material as obtained from annealing experiments at 60°C after irradiation with 24 GeV/c protons.

Fig 9b:

Damage parameters N_Y for oxygenated and standard material as obtained from annealing experiments at 60°C after irradiation with 24 GeV/c protons.

Fig 10a:

Current pulse shapes obtained after annealing for 8 min at 80°C on a proton irradiated oxygen enriched sample (835nm laser, front illumination).

Fig 10b:

Current pulse shapes obtained after annealing for 960 min at 80°C on a proton irradiated oxygen enriched sample (835nm laser, front illumination).

Fig 11:

Determination of depletion voltage from CCE-V (compare Fig.10a and 10b) and C_s -V measurements for two different annealing times.

Fig 12:

ΔN_{eff} extracted from C_s -V and CCE-V measurements.

Fig. 13:

Depletion voltage normalised to 300 μ m detector thickness as a function of gamma dose for 1.1 k Ω cm and 2.2 k Ω cm oxygenated and standard silicon detectors.

Fig 14a:

Damage projections for the B-Layer of the ATLAS Pixel Detector.

Fig 14b:

Damage projections for ATLAS strip detectors located 30cm from the interaction point.

Fig 15:

Isochronal annealing ($\Delta T = 20^\circ\text{C}$, $\Delta t = 20$ min) of DLTS spectra after radiation damage with $10^{11} < 5.3 \text{ MeV} >$ neutrons per cm^2 (3 k Ω cm n-type epitaxial material).

Fig 16:

DLTS spectra (normalised to introduction rate at 200K) obtained after irradiation with neutrons and a subsequent 80 min heat treatment at 60°C for different materials (see legend).

Fig 17:

DLTS spectra obtained on samples from the same wafer obtained after irradiation with different particles (see legend) and a 80 min lasting heat treatment at 60°C. The spectra are normalised to the 1 MeV neutron equivalent introduction rate at 200 K.

Fig 18a:

Evolution of the DLTS spectrum at 60°C for a neutron irradiated sample produced from Cz silicon.

Fig 18b:

Correlation between trap E4b and leakage current.

Fig 19:

Relative damage efficiency for different particles as function of recoil energy.

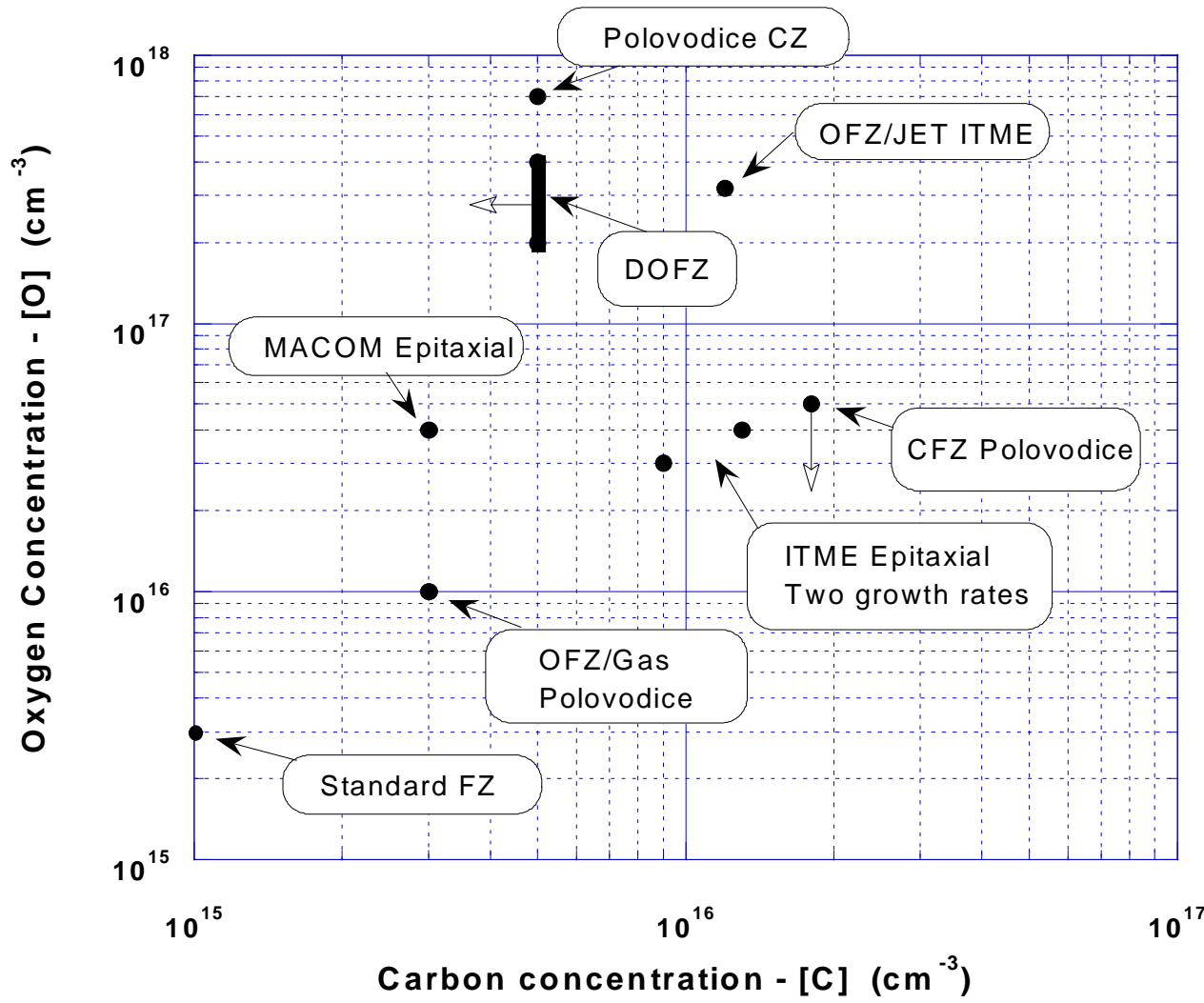


Fig. 1

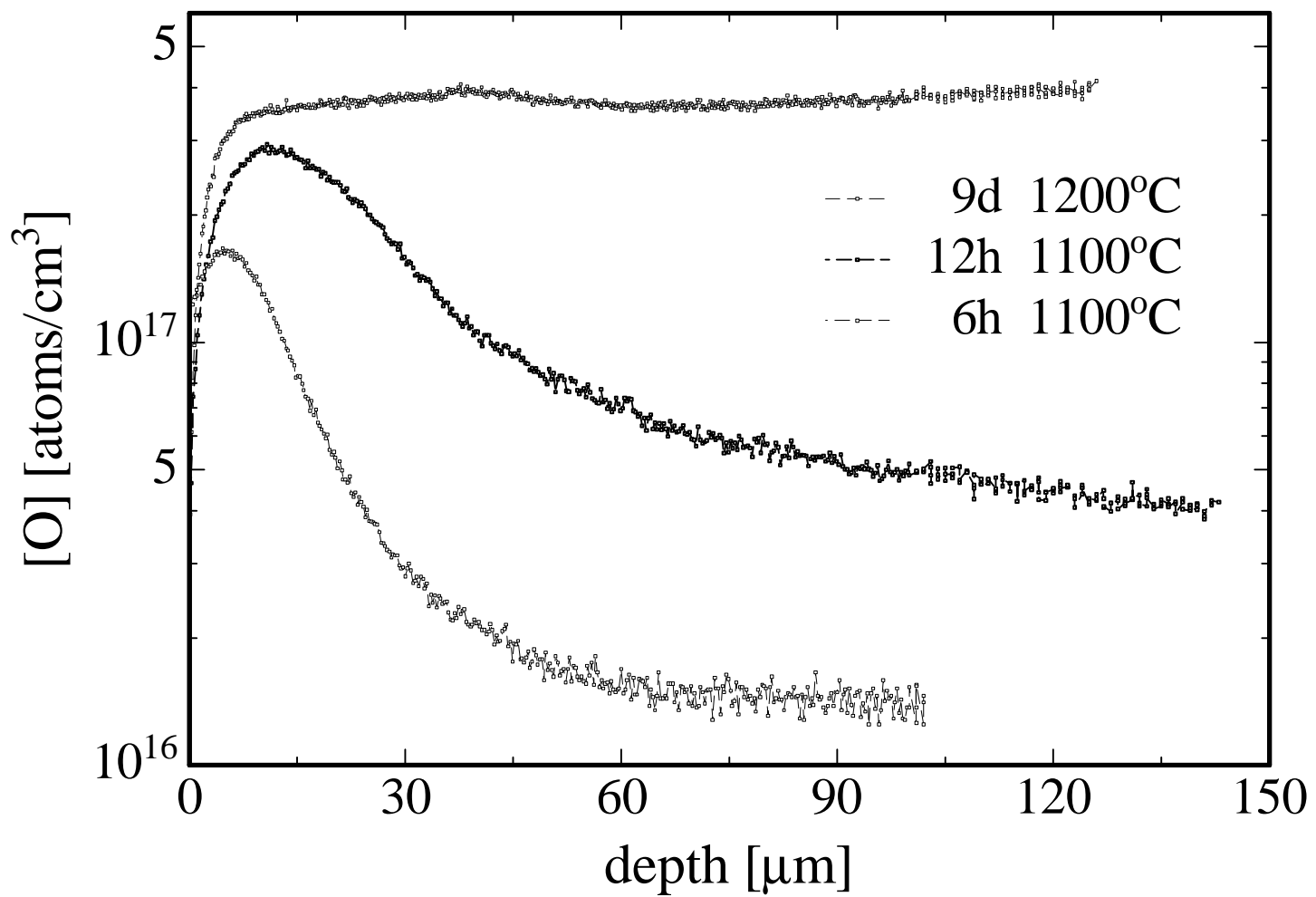


Fig. 2

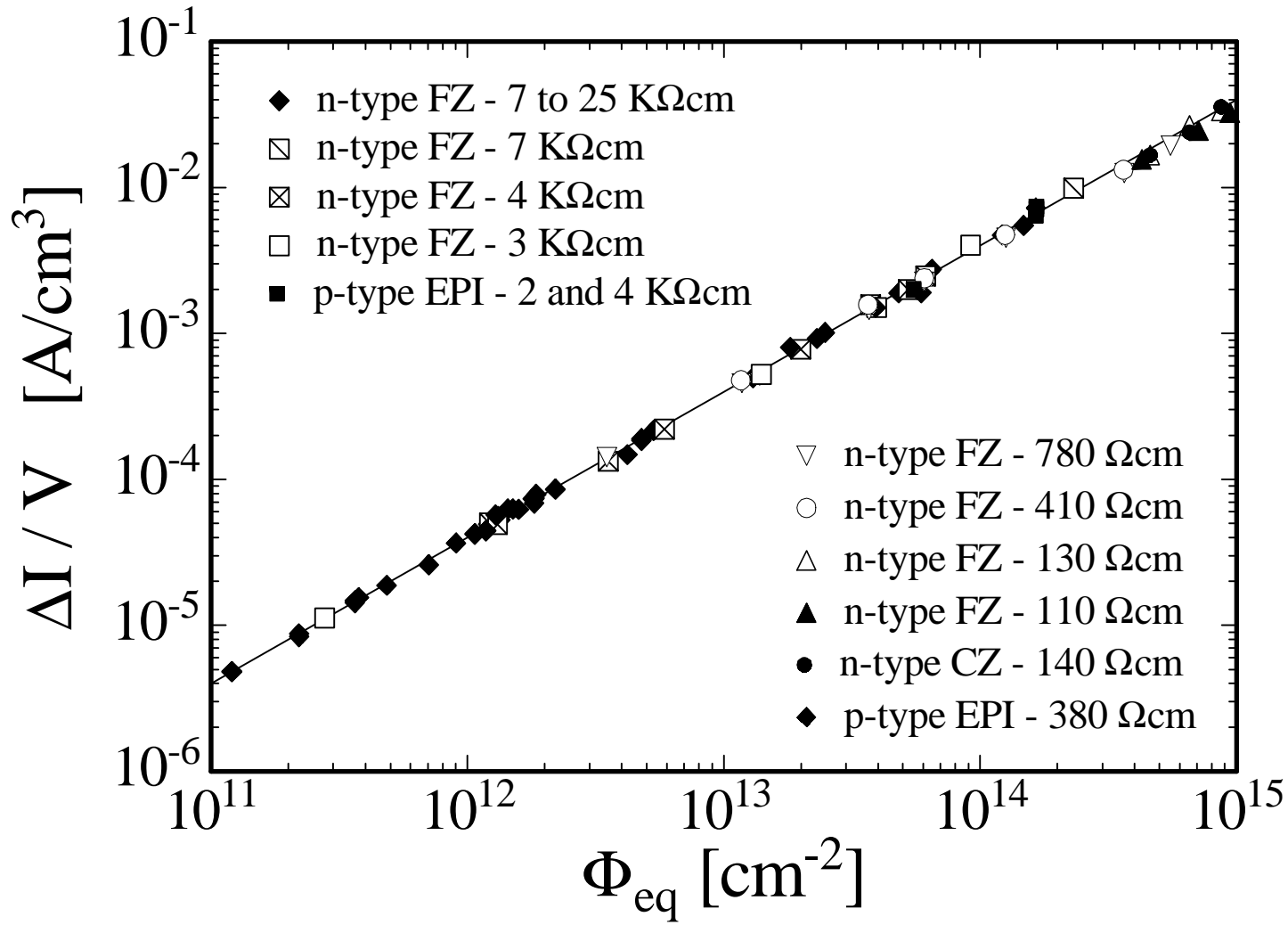


Fig. 3a

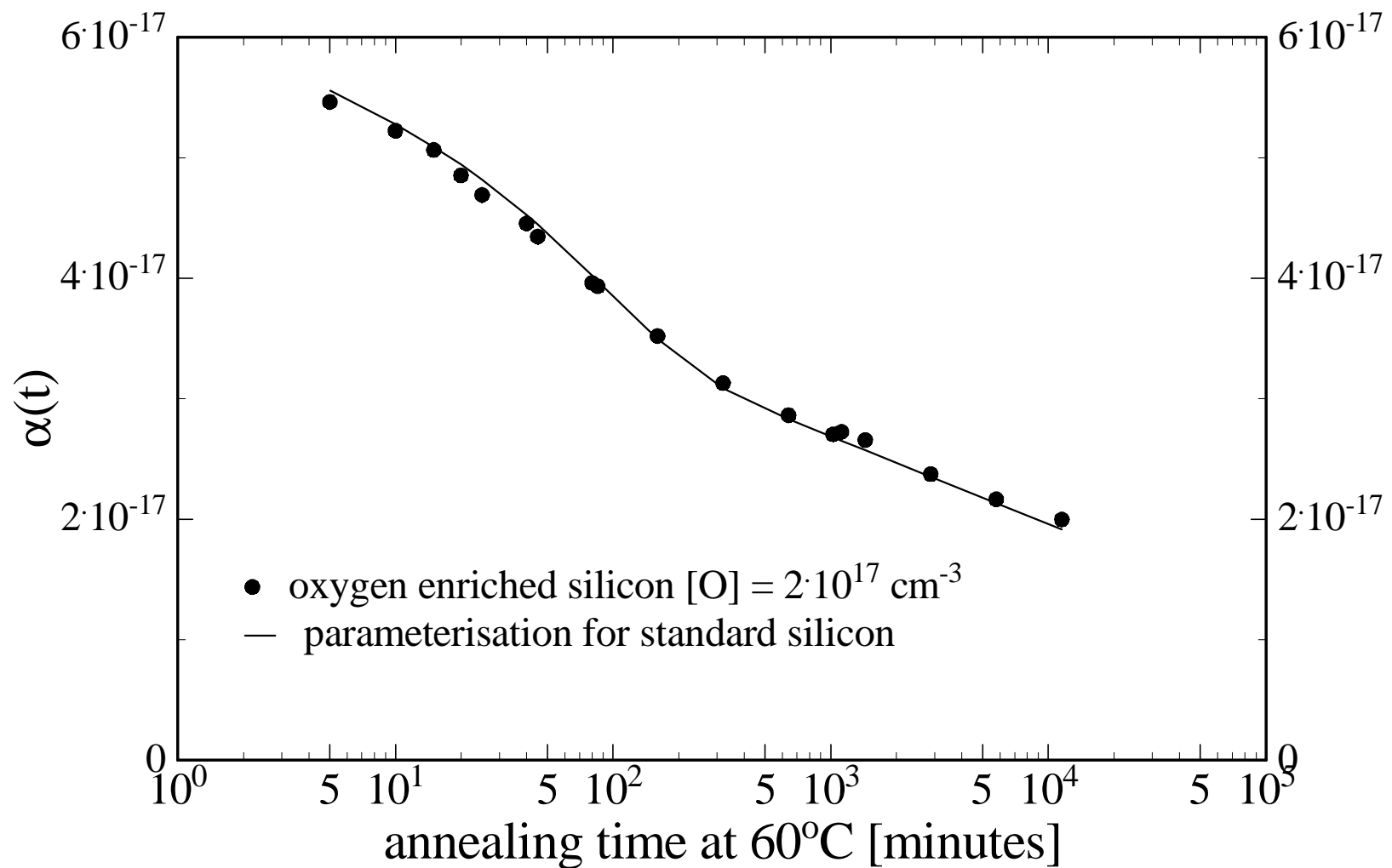


Fig 3b

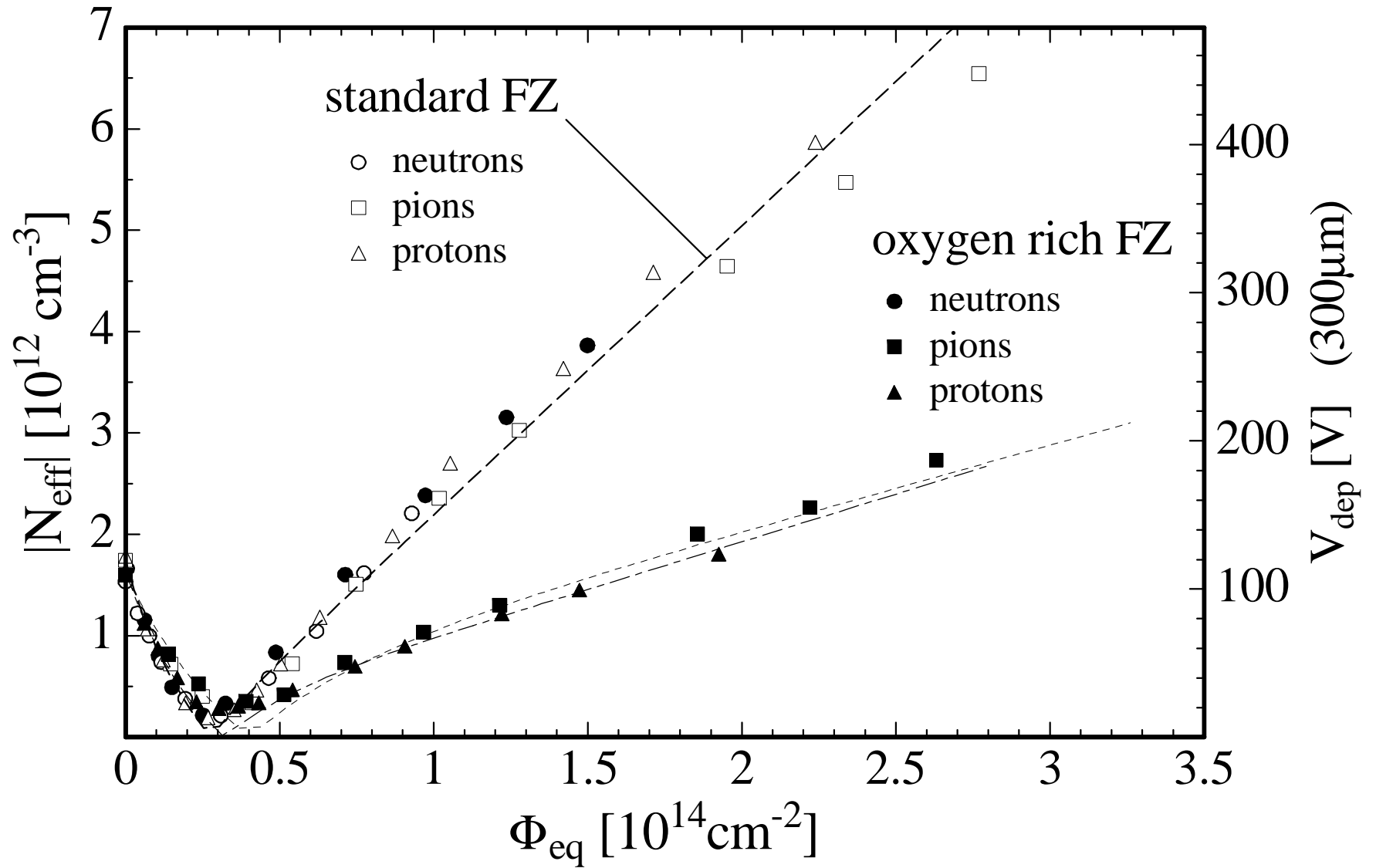


Fig. 4a

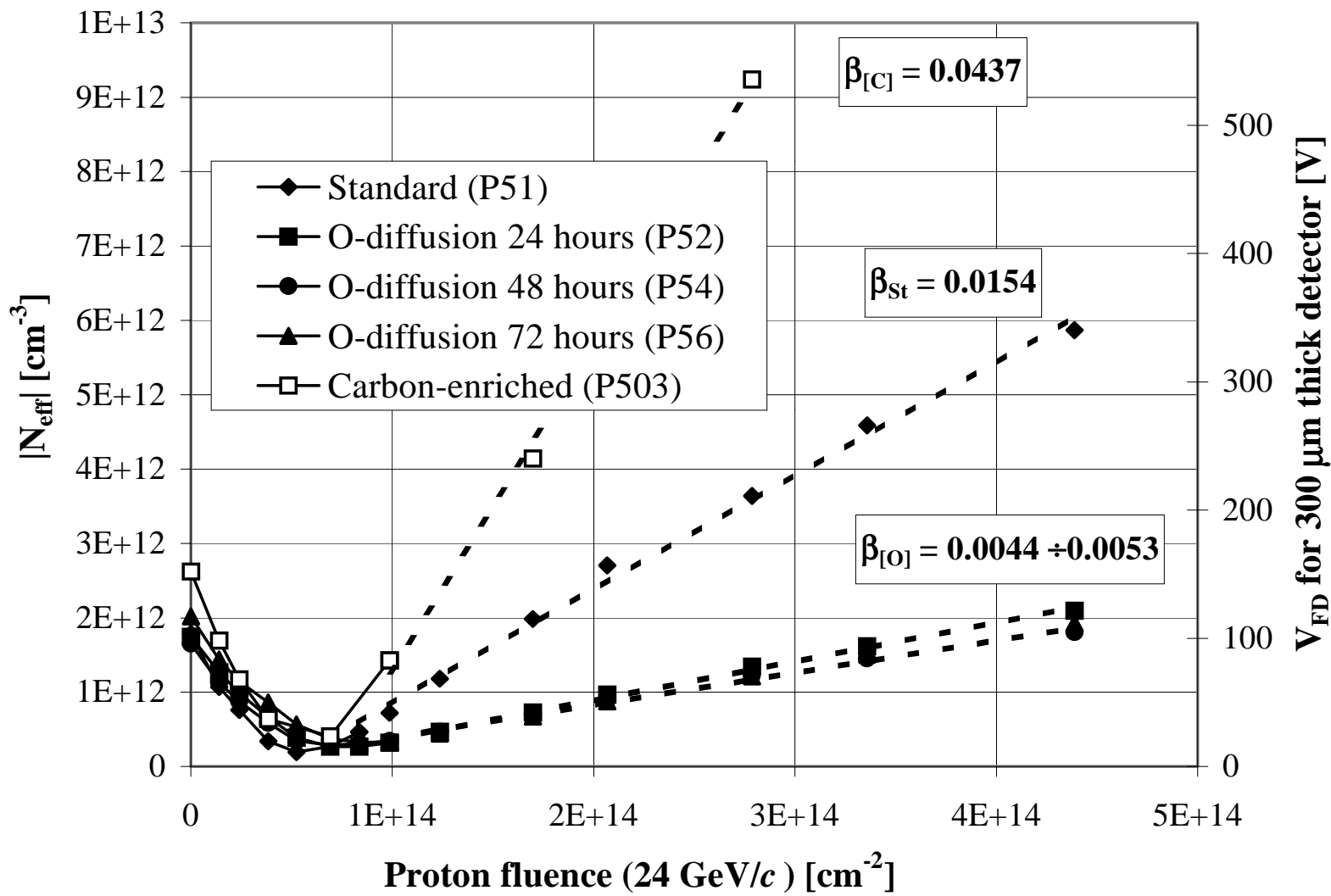


Fig. 4b

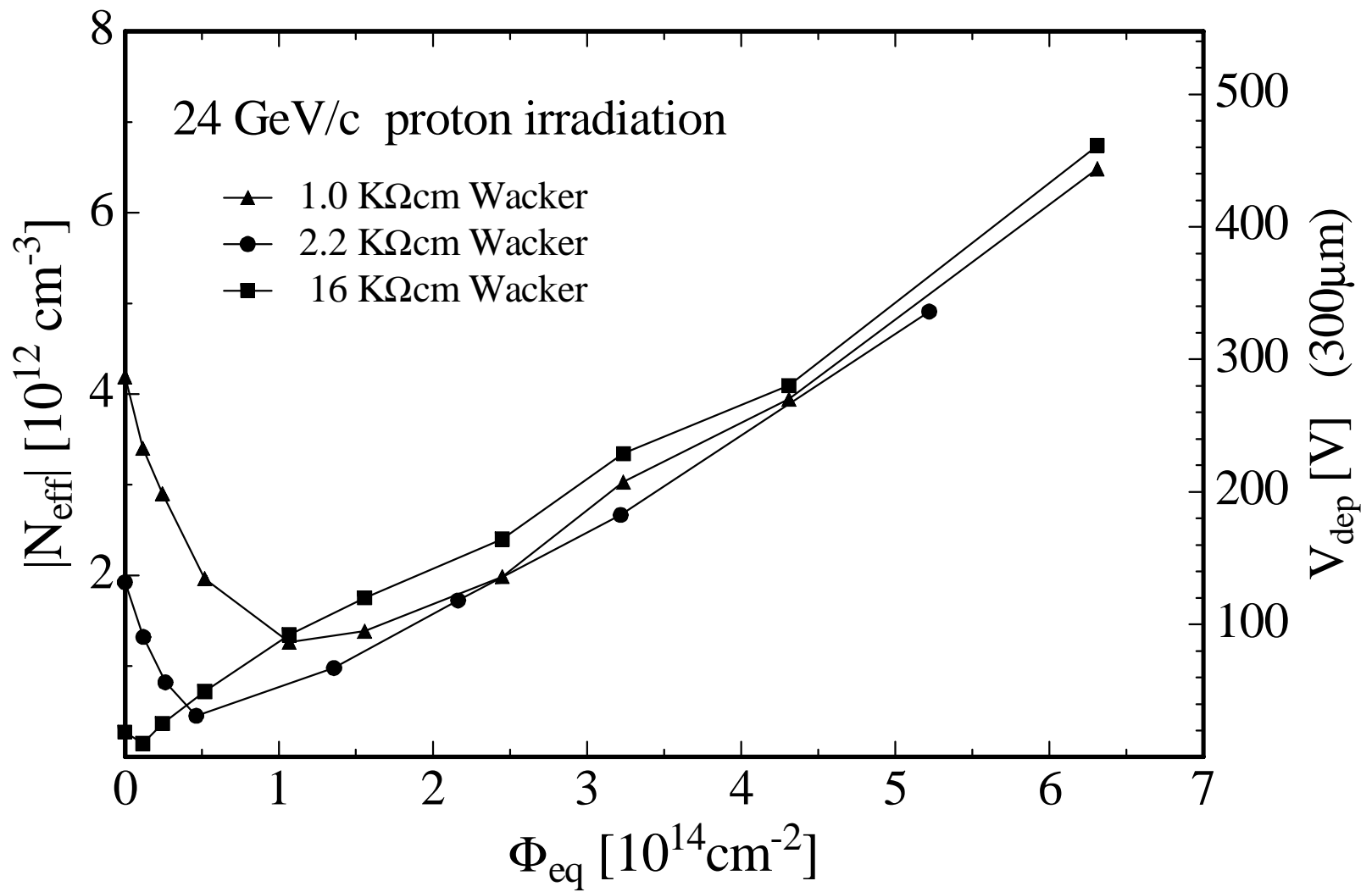


Fig. 5a

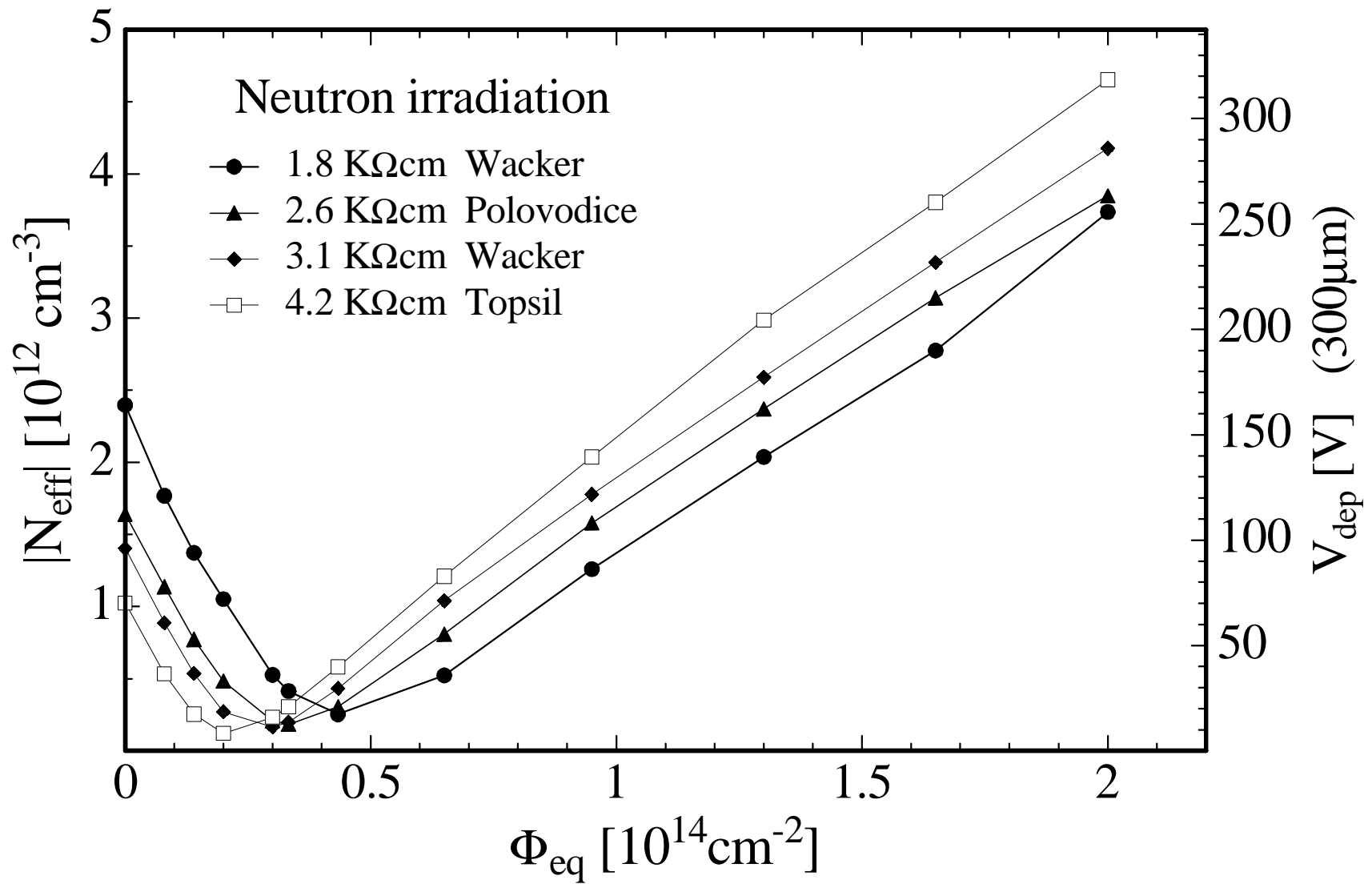


Fig. 5b

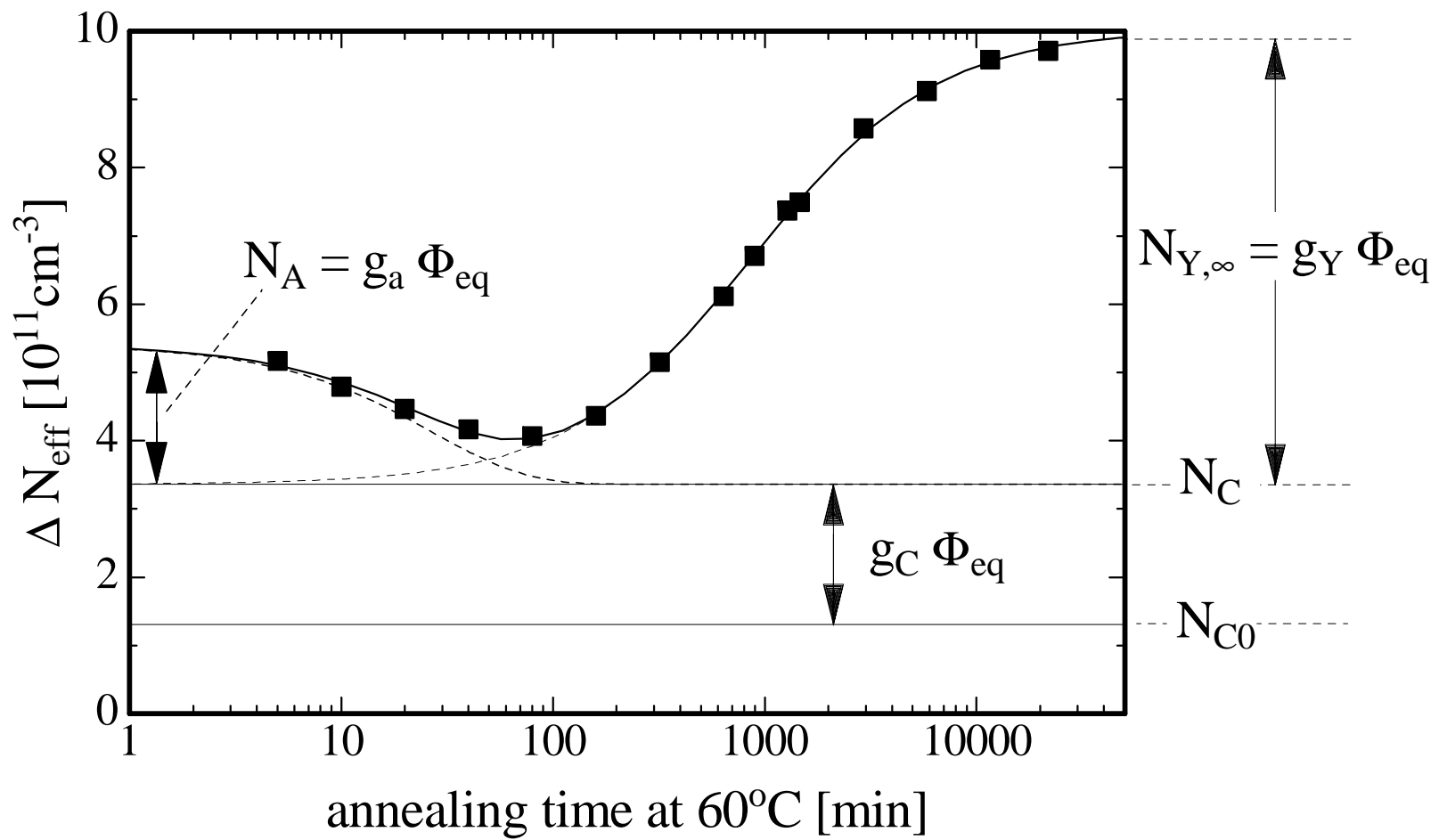


Fig. 6

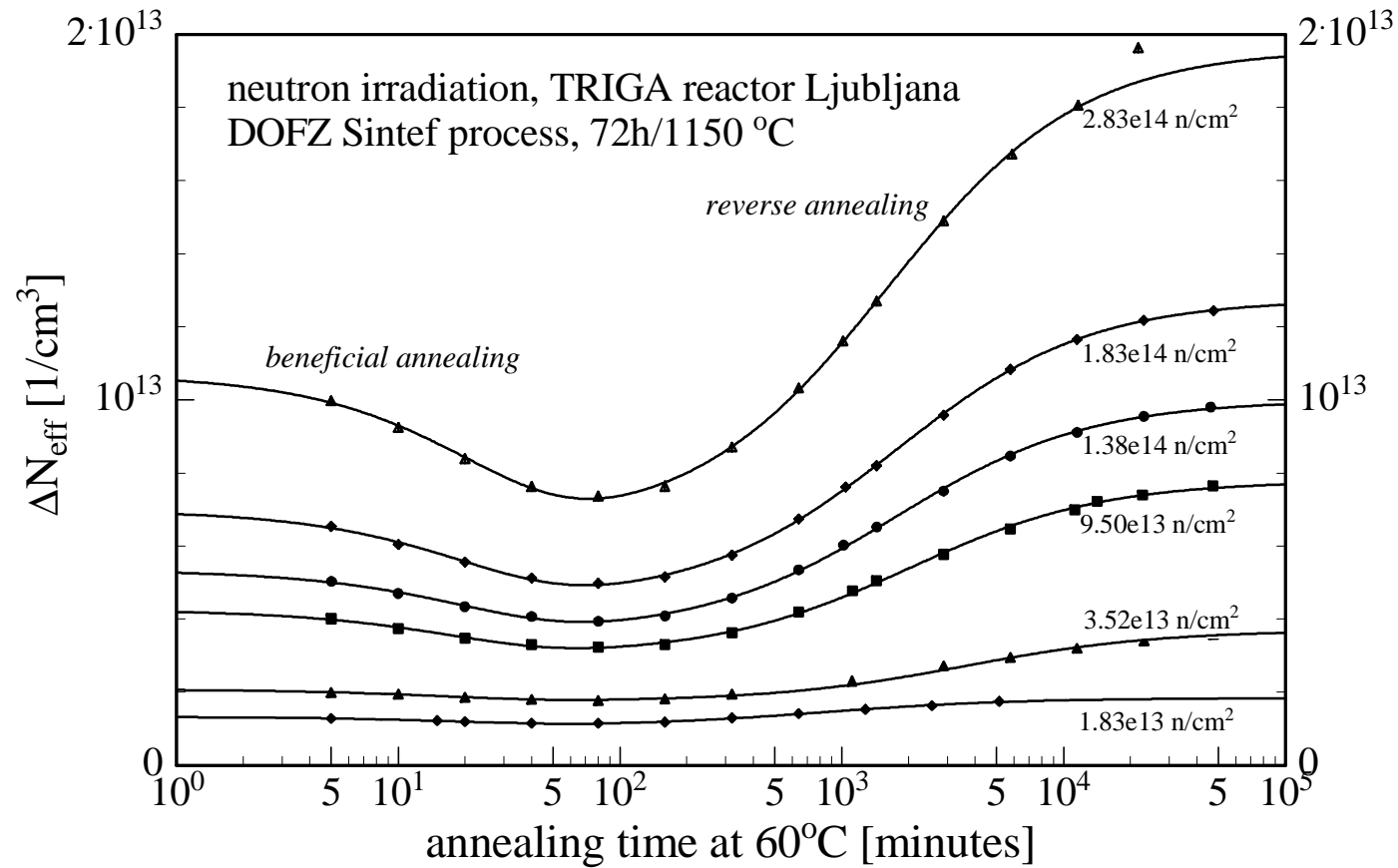


Fig. 7

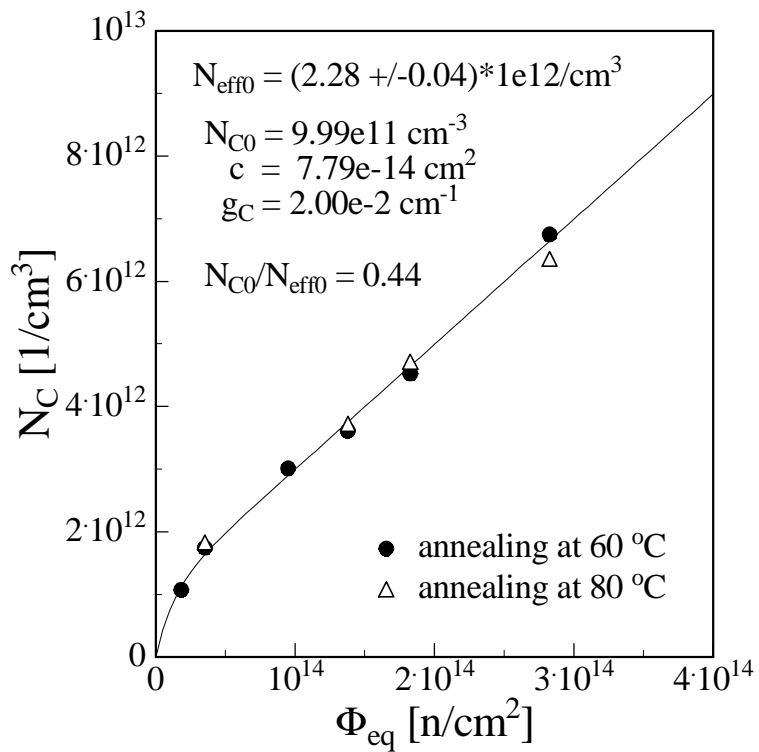


Fig. 8a

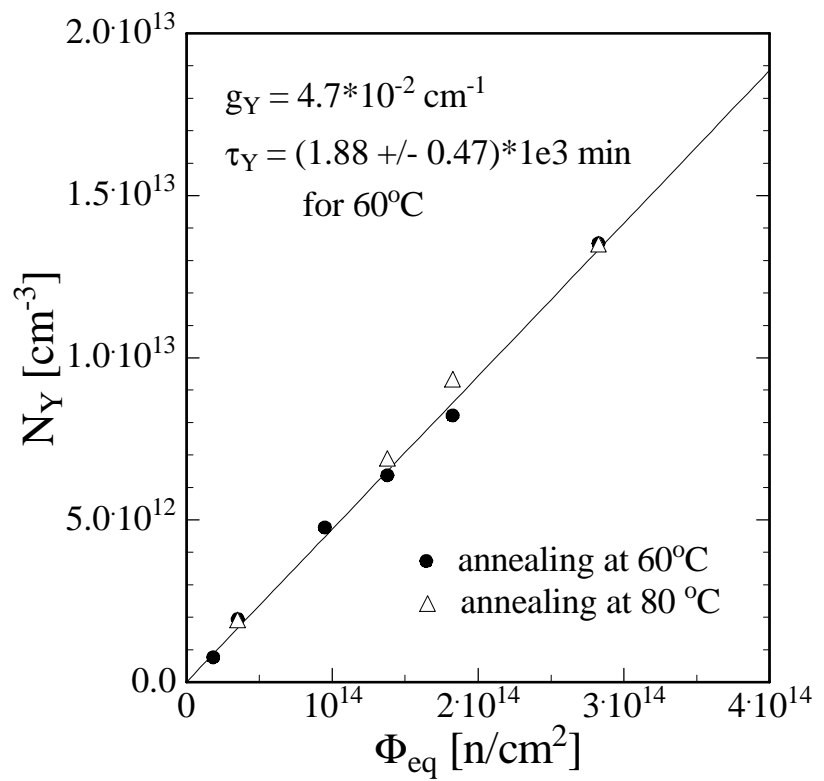


Fig 8b

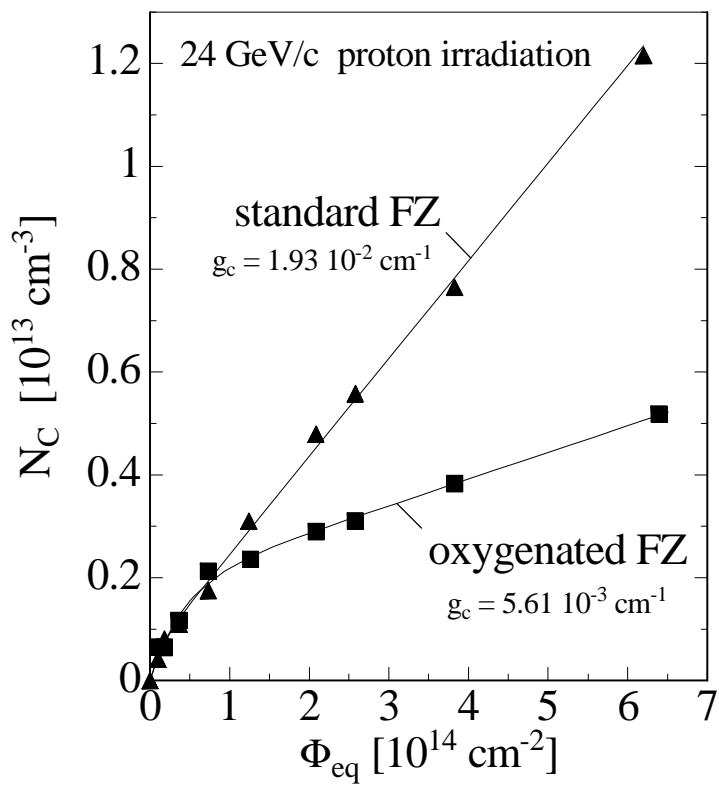


Fig. 9a

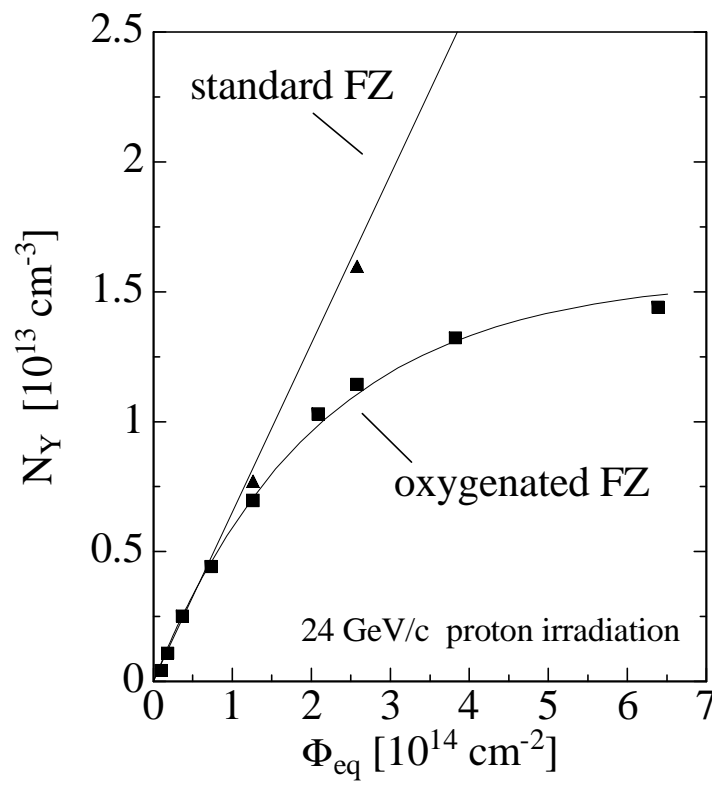


Fig 9b

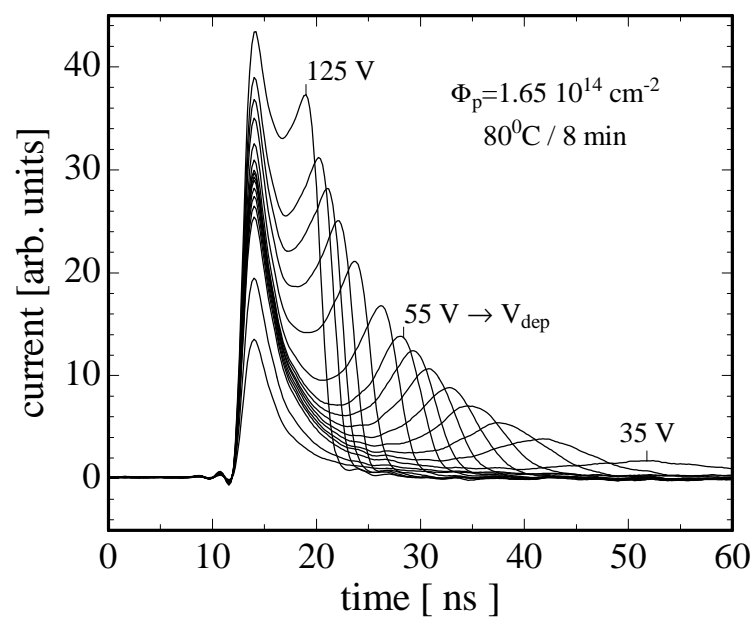


Fig. 10a

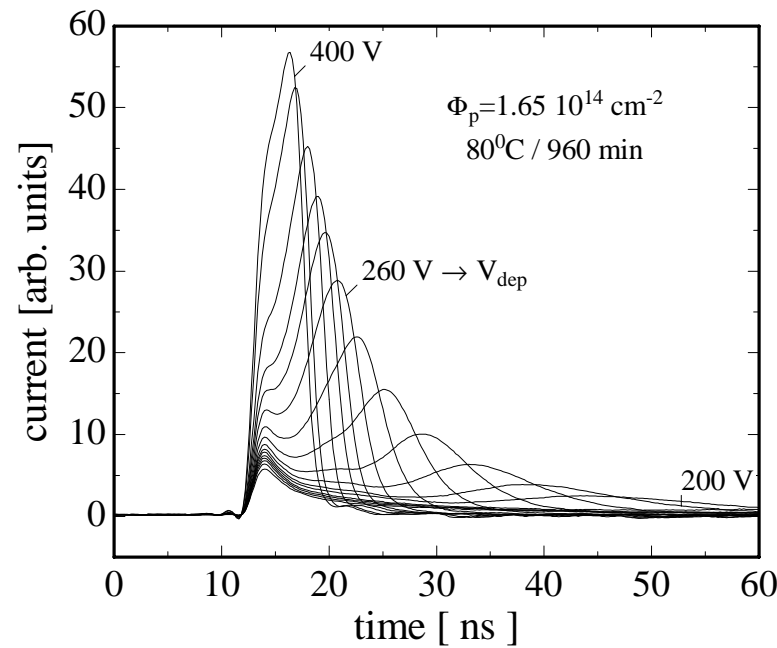


Fig 10b

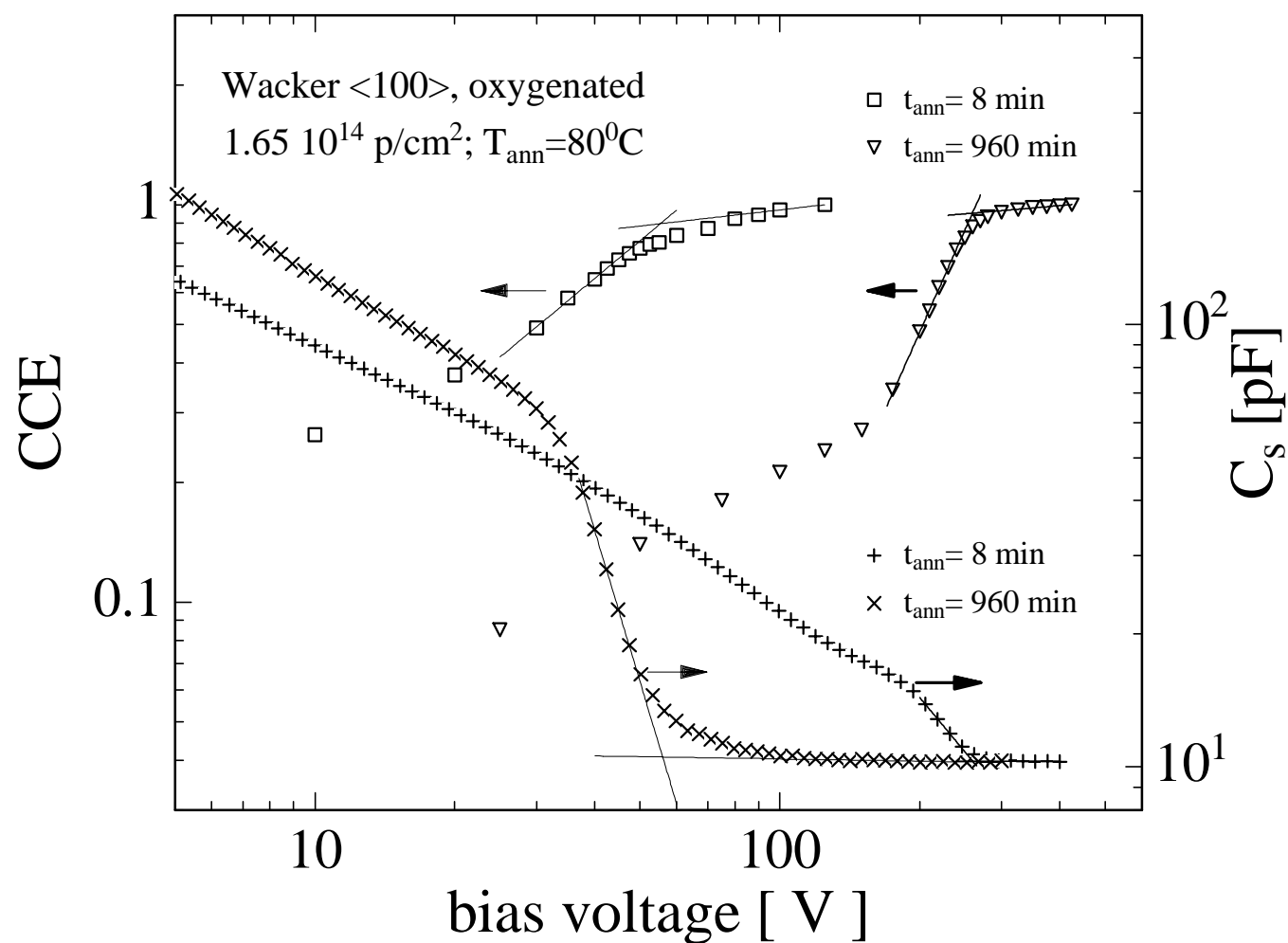


Fig. 11

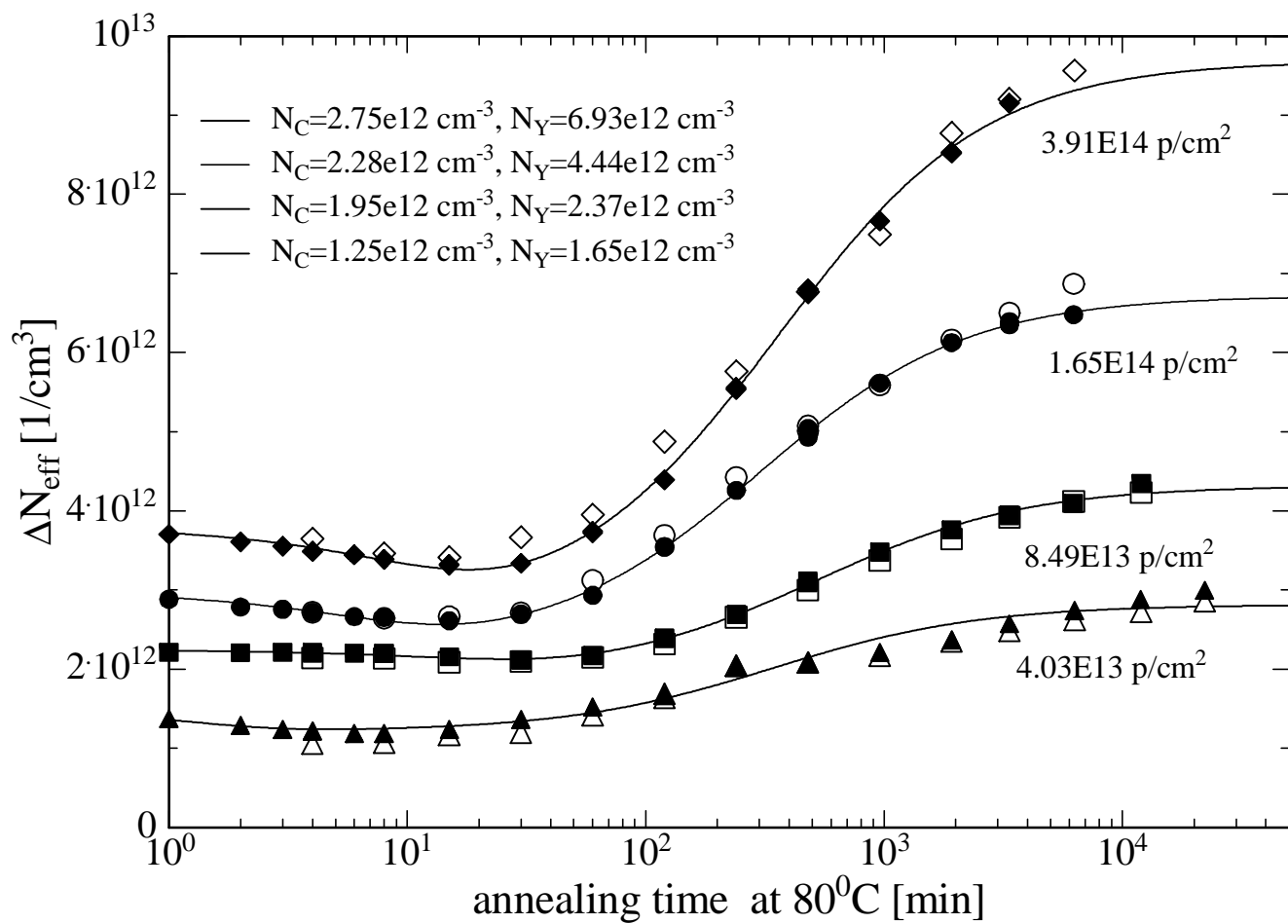


Fig. 12

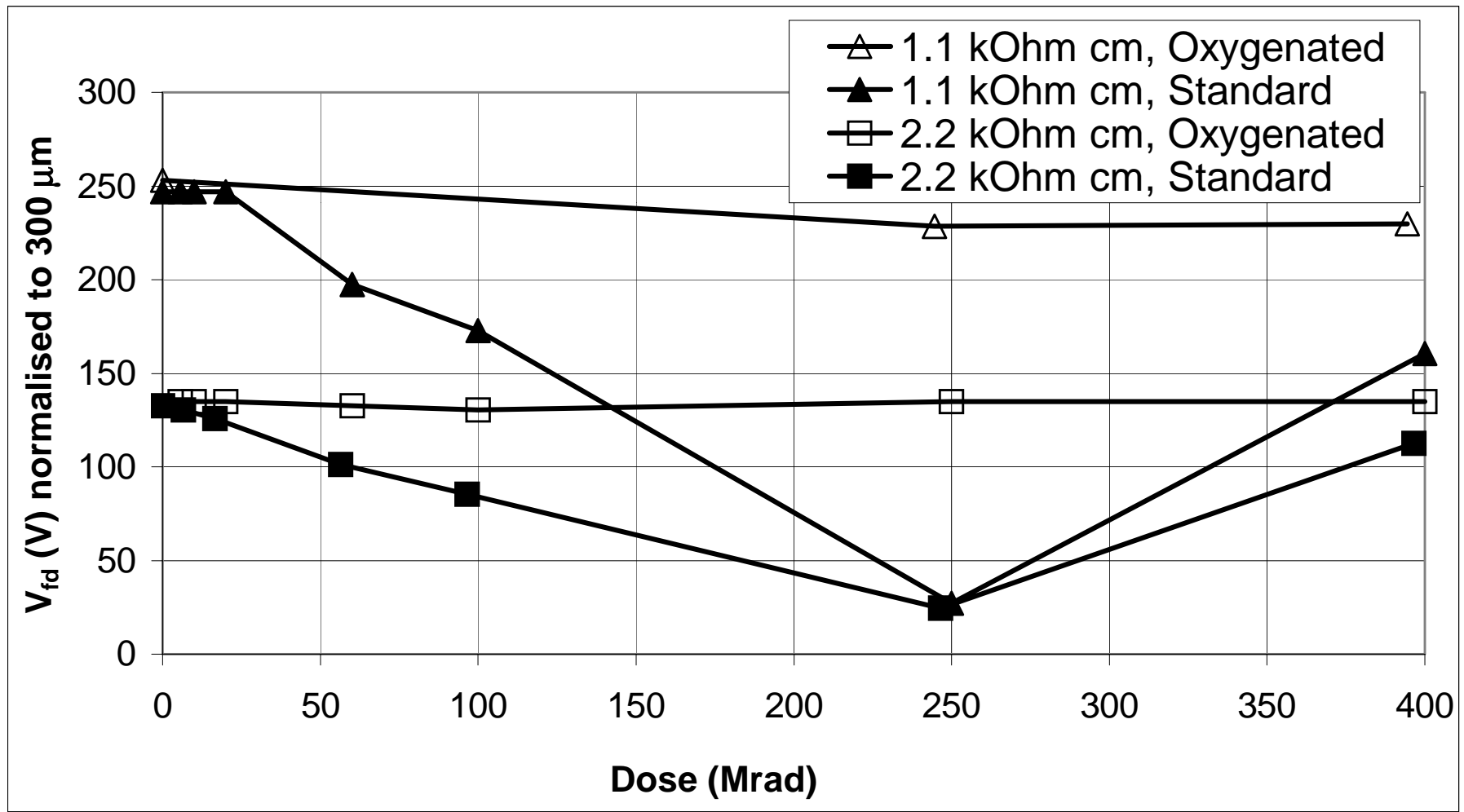


Fig.13:

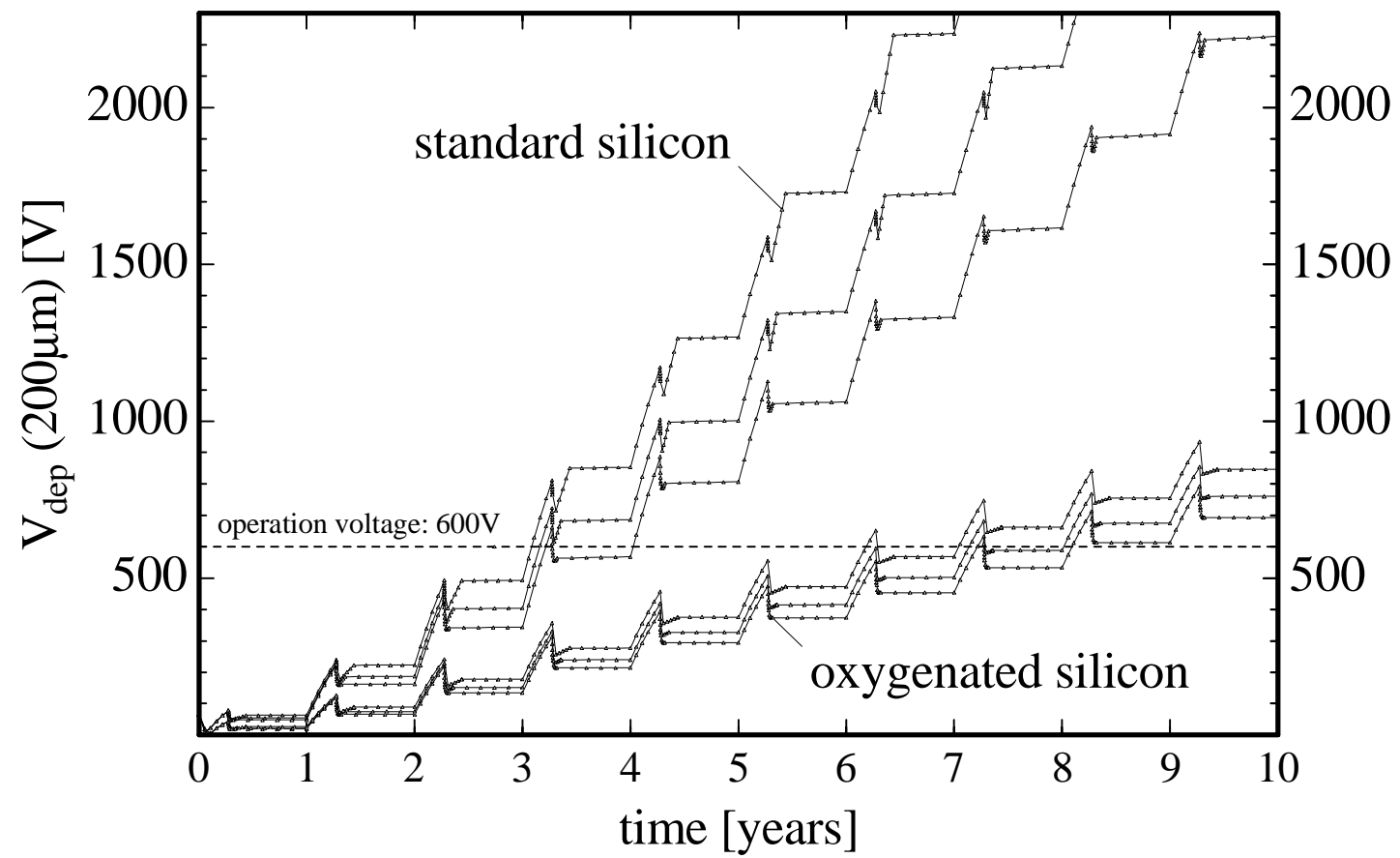


Fig. 14a

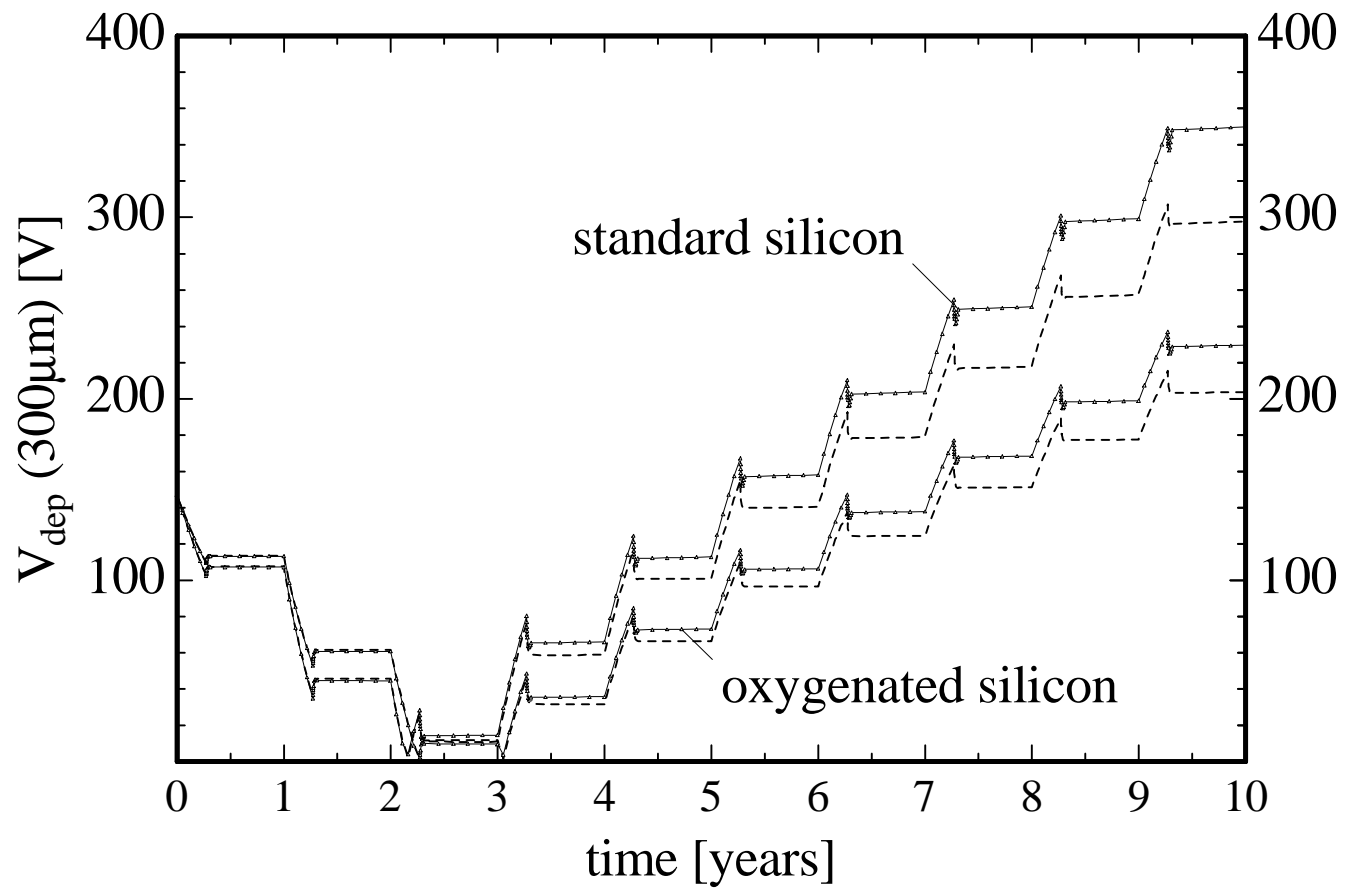


Fig. 14b

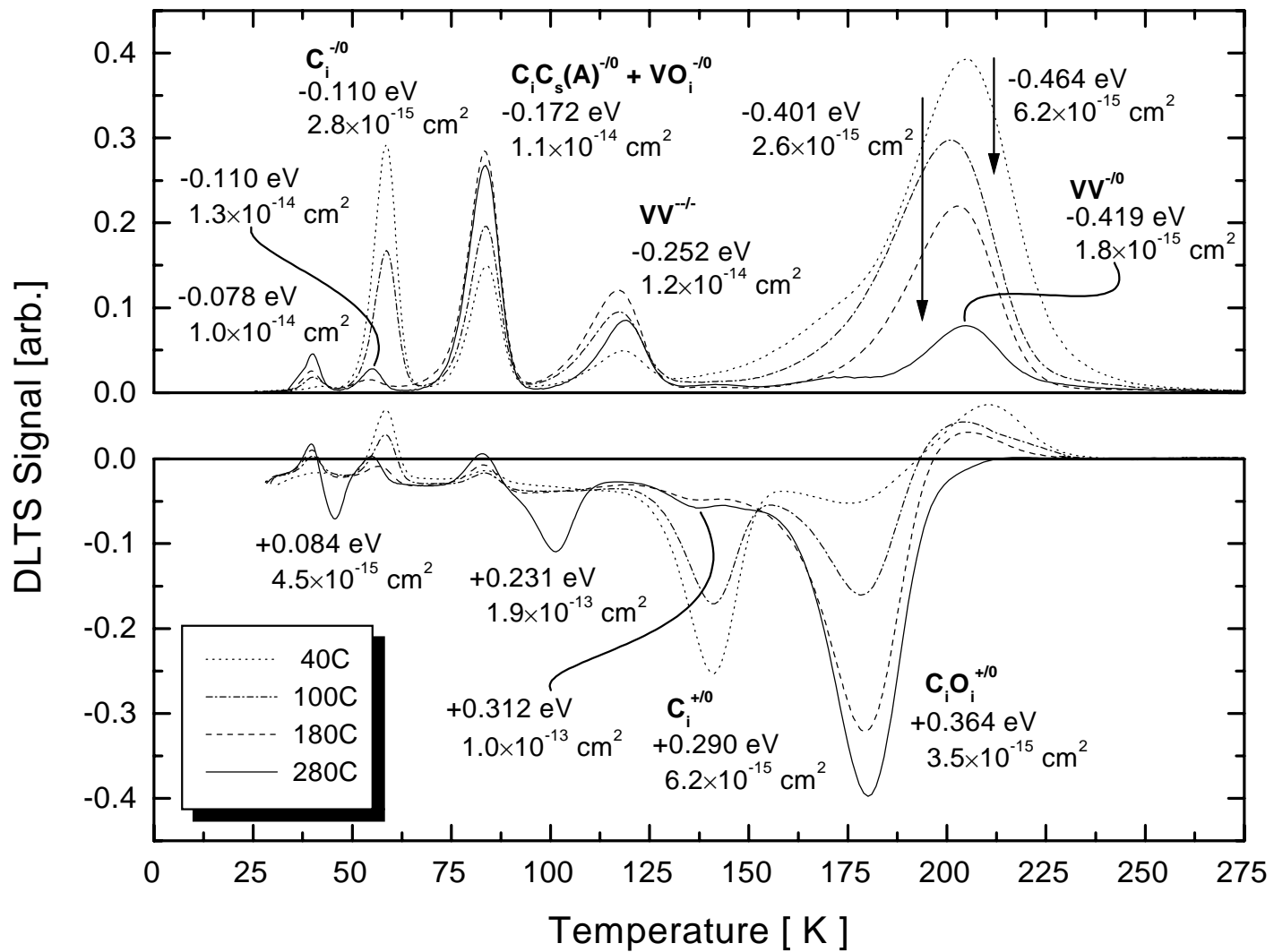


Fig. 15

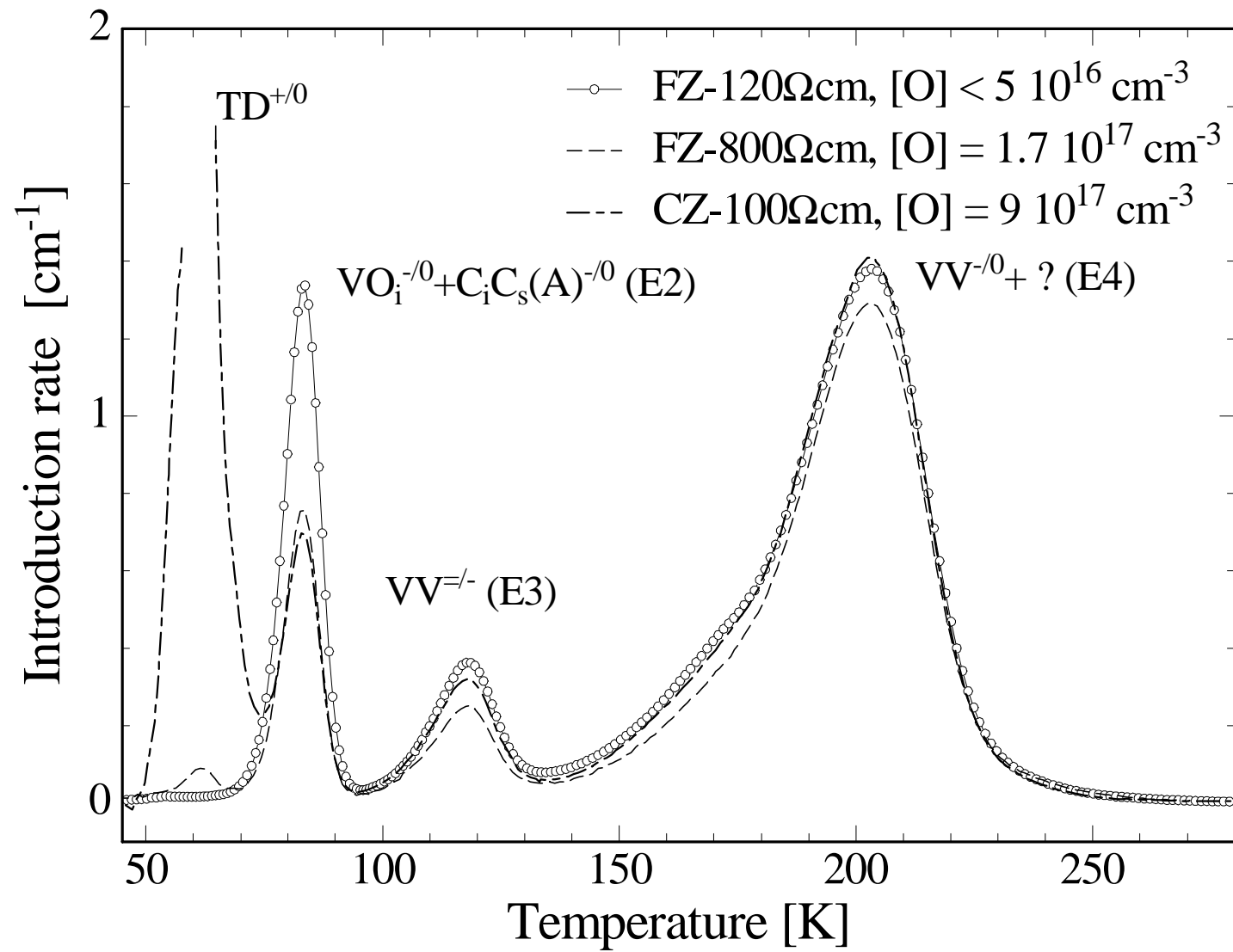


Fig. 16

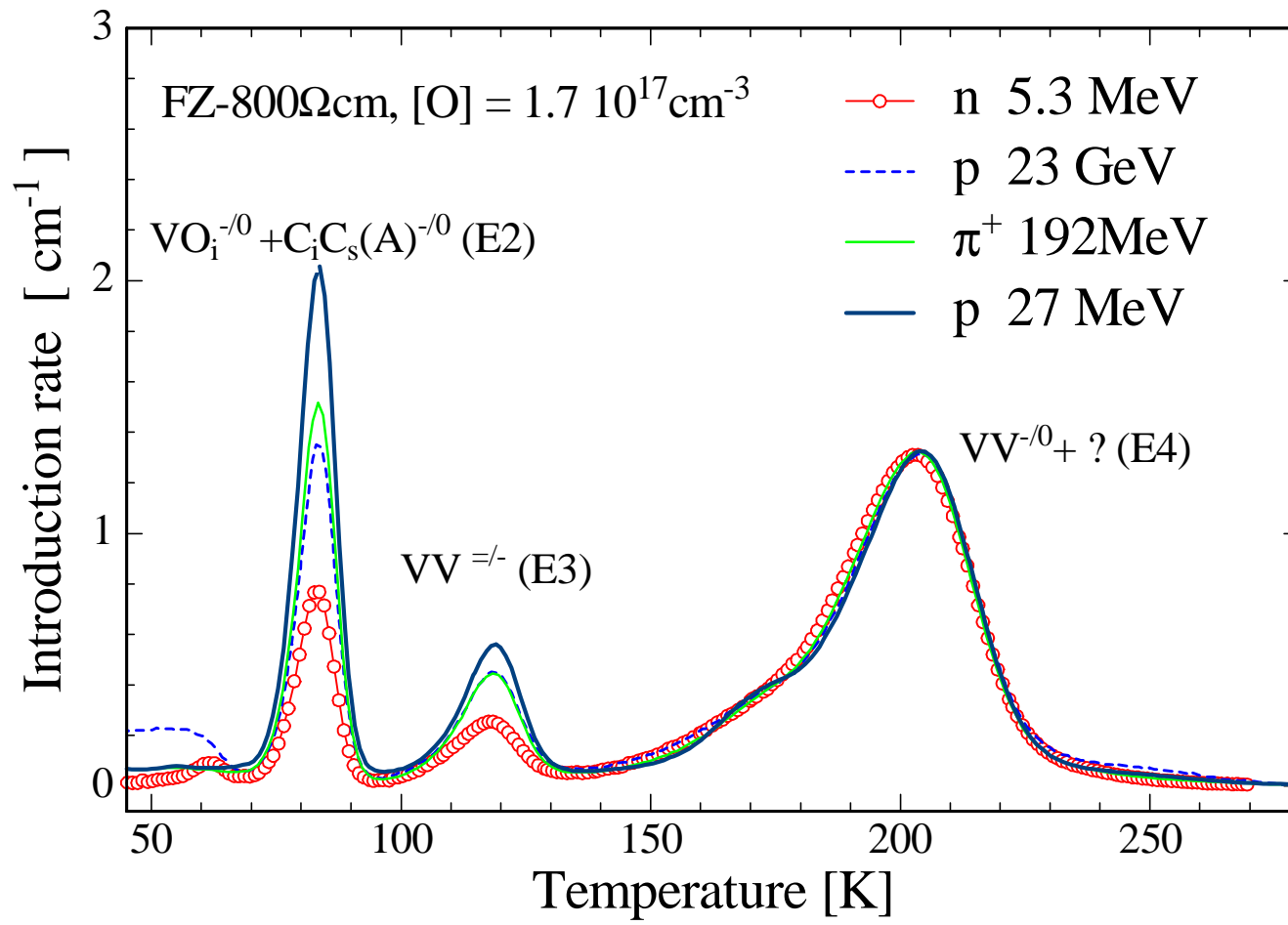


Fig. 17

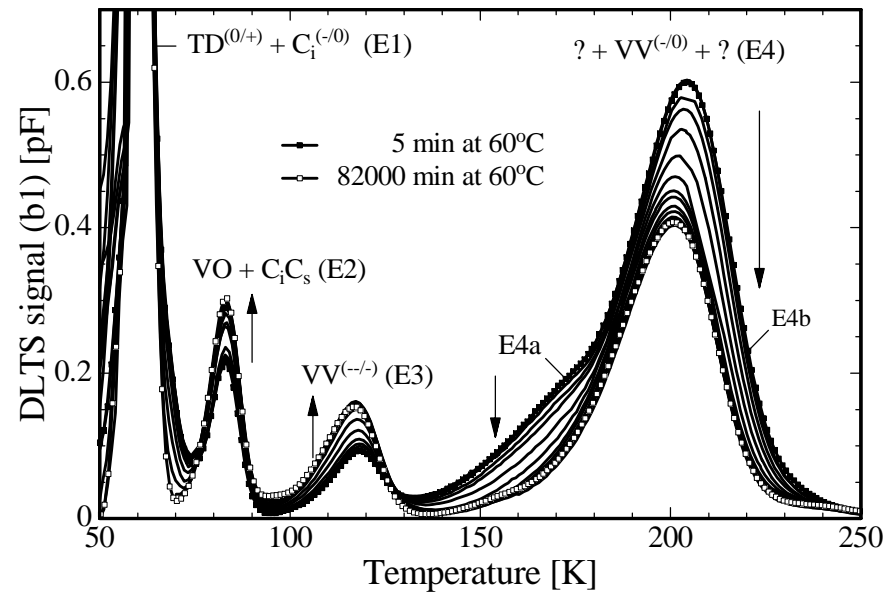


Fig. 18a

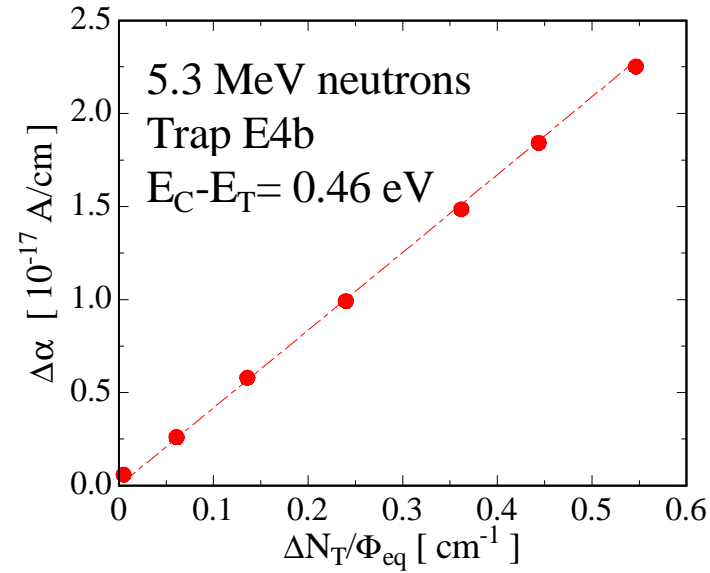


Fig18b

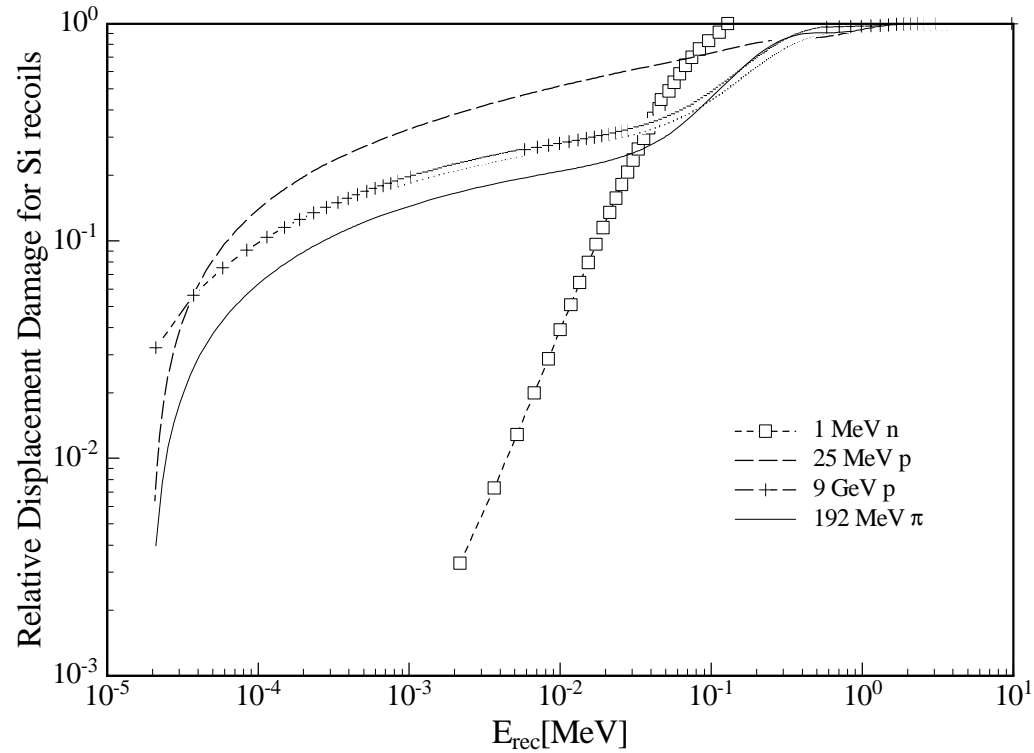


Fig. 19